

Nonlinear ac response of the vortex system in the cubic (K, Ba)BiO₃ superconductor

A. Conde-Gallardo^{1,2}, I. Joumard¹, J. Marcus¹, and T. Klein^{1,a}

¹ Laboratoire d'Études des Propriétés Électroniques des Solides, Centre National de la Recherche Scientifique, B.P. 166, 38042 Grenoble Cedex 9, France

² Departamento de Física, CINVESTAV-IPN, Apdo, Postal 14-740, Mexico D.F. 07300, Mexico

Received 17 March 1999

Abstract. We present ac susceptibility measurements performed on (K, Ba)BiO₃ single crystals with different geometries: thick films, bars and hollow cylinders. We show that the h_{ac} dependence of the real (χ') and imaginary (χ'') parts of the ac susceptibility is in very good agreement with Brandt's numerical calculations (Phys. Rev. B **58**, 6523 (1998)) in the modified Bean critical state. Creep effects (at $H_{dc} = 0.3T$) are investigated by studying the frequency dependence of the current density deduced from the temperature scans of the ac susceptibility over a large frequency range ($0.02 \text{ Hz} < \omega < 2000 \text{ Hz}$). The relaxation rate $S = d\ln(J)/d\ln(\omega) \sim 4\%$ is temperature independent and very similar to the one usually obtained in high T_c cuprates.

PACS. 74.60.Ge Flux pinning, flux creep, and flux-line lattice dynamics – 74.60.Ec Mixed state, critical fields, and surface sheath – 74.25.Nf Response to electromagnetic fields (nuclear magnetic resonance, surface impedance, etc.)

1 Introduction

The vortex creep phenomena in high T_c superconductors have been extensively studied over the last ten years but still remain a very controversial issue [1]. The vortex dynamics is most commonly investigated either by measuring the relaxation of the dc magnetization with time or equivalently the frequency dependence of the response of the vortices to ac fields. ac susceptibility measurements can indeed be used as a very powerful tool in the verification of models for both *creep* and *pinning* in the mixed state of type II superconductors. Many theoretical papers have thus been devoted to the ac response of superconducting samples either in Bean critical state [2–4] (*i.e.* for bulk pinning) or in the presence of large shielding currents flowing near the sample edges [5, 6] (*i.e.* for surface and/or geometrical barrier pinning). The latter model has hence been successfully applied to high quality BiSrCaCuO samples [7, 8] whereas the ac response of YBaCuO films could be better described by the bulk pinning model [9].

A complete description of the ac response of superconductors of arbitrary shape in presence of large creep phenomena is a tremendous task which has not been completely addressed yet. The nonlinear equations can usually not be solved analytically but numerical calculations have been performed for various geometries and creep models [10–12]. The ac response has, for instance, been computed

by Brandt for rings, thin disks (in transverse magnetic field) [10] and, very recently, bars and cylinders with arbitrary length [11] assuming that the electrical field E is related to the current density J through: $E \sim J^n$. Such a $E - J$ characteristic may be used to mimic arbitrary creep phenomena by varying the n exponent from 1 (Ohmic response) to ∞ (Bean model).

The aim of this paper is to present a detailed characterization of the ac response of the (K, Ba)BiO₃ superconductor ($T_c \sim 30 \text{ K}$). This *cubic* system presents a vortex phenomenology which is very similar to the one observed in high T_c cuprates including the presence of a vortex liquid phase (despite much smaller thermal fluctuations [13]), a “fishtail” effect in the magnetization loops [14] and relaxation phenomena [15]. However, in contrast to high T_c cuprates, its crystallographic structure is perfectly isotropic and its $H - T$ phase diagram remains experimentally accessible down to the lowest temperatures ($H_{c2} < 30T$ [16]). The paper is organized as follows. The sample preparation and experimental procedure is briefly described in Section 2. The origin of pinning is investigated in Section 3 by varying the amplitude of the ac field at fixed frequency. The experimental data are compared to the numerical calculations performed by Brandt for three different geometries and we will show that the ac response can be well described by the *bulk pinning* model. Finally, creep effects have been studied by varying the frequency of the ac field from 0.02 Hz to 2 kHz (Sect. 4). We will

^a e-mail: klein@lepes.polycnrs-gre.fr

show that the frequency dependence of the current density can be directly deduced from $\chi'(T, \omega)$ and discuss this dependence in view of both $U \sim \ln J$ [17] and collective creep models [18].

2 Experimental and sample preparation

The ac susceptibility has been measured on three (K, Ba)BiO₃ single crystals grown by electrochemical crystallisation: (A) a thick film (thickness/width ~ 0.01) grown on the top of a BaBiO₃ substrate: $T_c = 28$ K, (B) a small (in order to avoid strong sample inhomogeneities related to non uniform potassium distribution) cube $\sim (300 \mu\text{m})^3$: $T_c = 25$ K and (C) a “hollow square” cylinder obtained by coating a BaBiO₃ cubic seed by a superconducting (K, Ba)BiO₃ shell (we finally got an “hollow” cylinder by cutting out the top and bottom faces of the as-grown cube): $T_c = 31$ K. The different sample geometries are sketched out in the inset of Figures 1 and 2.

The magnetic field $B(T, h_{ac}, \omega)$ at the top of sample (A) and (B) has been measured with a Hall probe and the ac transmittivity T_H has been deduced from B using:

$$T_H(T) = \frac{B(T) - B(T \gg T_c)}{B(T \gg T_c) - B(T \ll T_c)}$$

for various amplitudes ($0.1 \text{ G} < h_{ac} < 20 \text{ G}$) and frequencies ($0.02 \text{ Hz} < f < 2 \text{ kHz}$) of ac modulation field. Note that we did not measure the *local* ac response that would be given by a miniature probe [19] much smaller than the sample size but an *average* response – *i.e.* the susceptibility – by using a rather large probe ($\sim (100 \mu\text{m})^2$ *i.e.* comparable to the sample size). The ac susceptibility of the “hollow” cylinder has been measured using an home made susceptometer at fixed frequency (1 kHz) for $0.03 \text{ G} < h_{ac} < 20 \text{ G}$. All samples presented a rather sharp superconducting transition ($\sim 1 \text{ K}$ at $h_{ac} = 0.1 \text{ G}$).

3 Evidence for bulk pinning

Figure 1 shows the real (χ') and imaginary (χ'') parts of the normalized susceptibility (at $\omega = 12 \text{ Hz}$) of the (K, Ba)BiO₃ thick film as a function of the reduced ac field h_{ac}/h_{max} (where h_{max} is the field corresponding to the maximum of dissipation). Seven temperatures between 23.5 K and 26.5 K have been reported as a single symbol. As expected from the nonlinear response theory, both $\chi'(h_{ac}/h_{max})$ and $\chi''(h_{ac}/h_{max})$ are temperature independent. Indeed, $h_{max} \sim Jd$ where J is the current density and d a characteristic length scale *i.e.* the radius for cylinders in a parallel geometry, the thickness for films in perpendicular field, and the ac susceptibility can be written as [10]:

$$\chi(h_{ac}, T, \omega) = F(h_{ac}/J(T, \omega)d) \quad (1)$$

where $F(x)$ depends on the sample geometry, pinning and creep mechanisms [20].

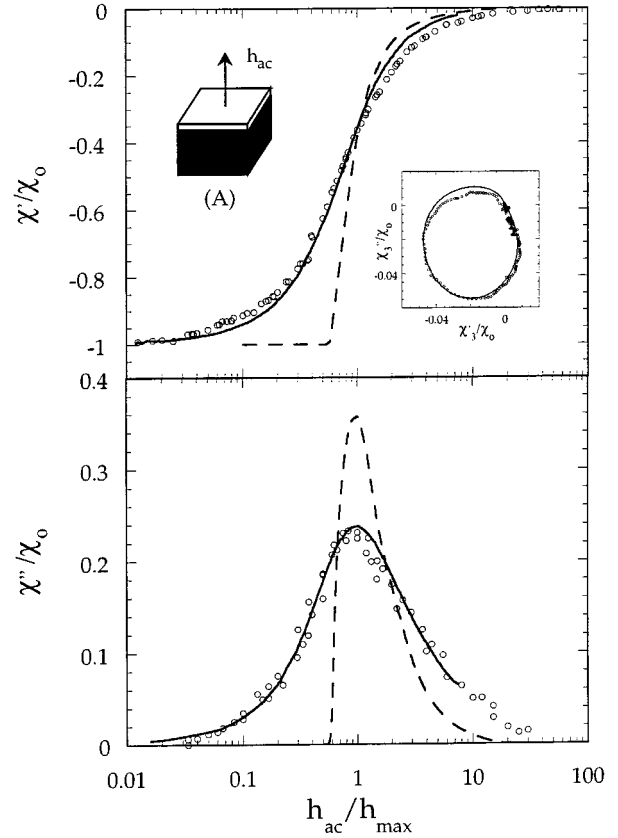


Fig. 1. h_{ac} field dependence of the real (χ') and imaginary (χ'') parts of the ac susceptibility of the (K, Ba)BiO₃ thick film (seven temperatures have been reported as a single symbol). The solid and dashed lines are the theoretical calculations for bulk and surface pinning respectively. In the lower inset: Argand plot of the third harmonic showing that the hysteretic process is dominated by bulk pinning barriers (see text for details). In the upper inset: sketch of the (K, Ba)BiO₃ thick film (white) grown on the top of a BaBiO₃ substrate (dark gray). The orientation of the ac field is indicated by the arrow.

As shown in Figure 1 the experimental data are in good agreement (the small discrepancies will be discussed in Sect. 4) with the numerical calculation for thick disks [11] (the influence of the lateral shape is negligible) in the Bean critical state [21]. As a comparison, we have also reported the calculations for geometrical barrier pinning with the appropriate thickness/width ratio. Clearly this latter model only provides a very poor fit to the data for $h_{ac} < h_{max}$ [20]. The discrepancy is particularly clear for χ'' for which a maximum of 0.36 is predicted in clear disagreement with the experimental value ~ 0.23 .

Another major difference between edge and bulk currents is given by the shape of the Argand (*i.e.* polar) plot of the third harmonic. Indeed, this plot is expected to resemble a *full* cardioid for edge currents but, as a consequence of the lenticular shape of the hysteretic loop for small h_{ac} values, only a *half* cardioid for bulk currents [8] (the left part of the cardioid corresponds to large h_{ac}/Jd

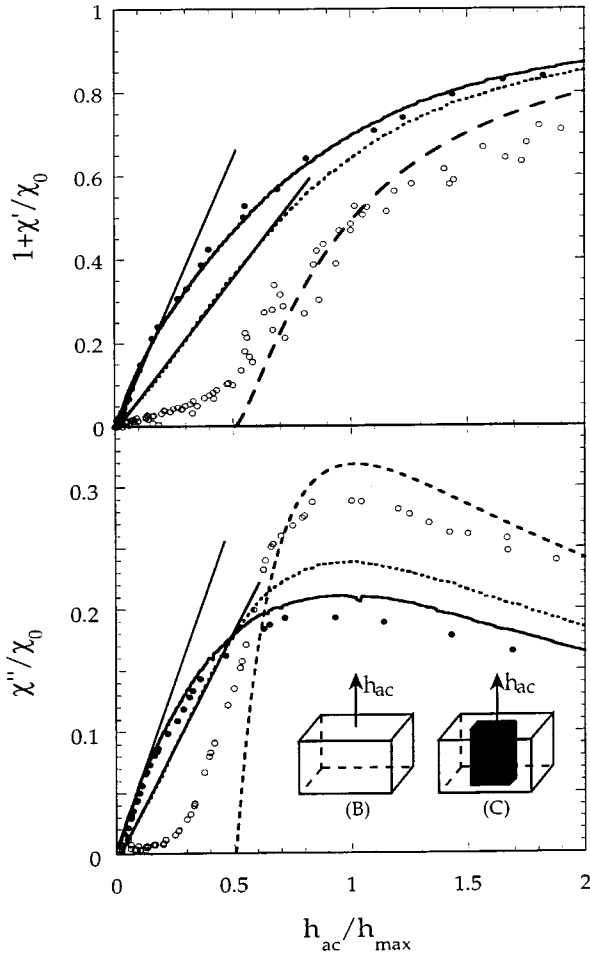


Fig. 2. h_{ac} field dependence of the real (χ') and imaginary (χ'') parts of the ac susceptibility of the (K, Ba)BiO₃ thick film (sample (A) – dotted line), cubic single crystal (sample (B) – solid circles) and hollow “cylinder” (sample (C) – open circles). The solid and dashed lines are the theoretical calculations for bars and thin walled cylinders respectively. In the lower inset: sketches of the cubic single crystal and hollow “cylinder” obtained by coating a BaBiO₃ seed (dark gray) with a superconducting (K, Ba)BiO₃ shell (white). The orientation of the ac field is indicated by the arrow.

values and is thus similar for both models [20]). As shown in the inset of Figure 1 the Argand plot of the (K, Ba)BiO₃ film is in very good agreement with the numerical calculations for thin disks in the bulk pinning model [2].

In order to emphasize the influence of the sample geometry on the ac response we have reported in Figure 2, the h_{ac} field dependence of the susceptibility for the three geometries (sample (A) – see Fig. 1 – has been reported as a dotted line). As shown the ac response of the cube is very similar to the one obtained for the thick film and is in good agreement with Brandt’s calculations for bars. As expected, the small h_{ac} field expansion of the real and imaginary parts of the susceptibility is linear for both geometries [11] and the $\frac{\chi''}{1+\chi'}$ ratio is independent of the sam-

ple thickness (note that a quadratic behavior would have been expected for thin films): we got $\frac{\chi''}{1+\chi'} = \frac{0.36}{0.84} = 0.43$ and $\frac{1.33}{0.55} = 0.41$ for sample (A) and (B) respectively in good agreement with the theoretical value ($\frac{4}{3\pi} = 0.42$).

On the other hand, a completely different behavior is obtained for the “hollow” cylinder (sample (C)). Indeed, for thin walled cylinders and planar rings [10] the screening remains perfect – *i.e.* no magnetic field penetrates the tube ($\chi' = -1$ and $\chi'' = 0$) – until h_{ac} reaches some critical value $H_p \sim h_{max}/2$. The magnetic field remains constant for higher h_{ac} values and the hysteresis loop is thus perfectly parallelogramic (the ac response of the ring is somehow similar to the one obtained for edge currents in presence of surface barrier pinning even though it is related to a very different physical origin). The “singularity” at H_p gradually disappears as the internal/external radius ratio tends towards zero but is still clearly visible for our “hollow” cylinder ($a_{int}/a_{ext} \sim 0.6$) which show a sharp drop in both χ' and χ'' for $h_{ac} < h_{max}$ (the dashed lines correspond to the numerical calculations for thin walled cylinders). Note also that the maximum in χ'' rises up to ~ 0.3 in good agreement with the numerical calculations.

4 Creep effects

High T_c superconductors are known to present large flux creep effects and it is thus necessary to include those phenomena to get a complete description of the ac response. A first indication for creep effects in our samples is actually given by the h_{ac} dependence of the susceptibility at fixed frequency. Indeed, as shown in the inset of Figure 3, the experimental data are better described by the numerical calculations for $n \sim 11$ than by the Bean limit. However, the difference in the χ' *vs.* h_{ac}/h_{max} curves between $n = 11$ and $n = \infty$ is small and it is thus necessary to measure the frequency dependence of the ac response in order to get a better description of the creep process. The influence of the frequency of the ac field on the susceptibility of the thick film (at $h_{ac} = 10$ G, $H_{dc} = 0.3T$) is presented in Figure 3. As shown, the $\chi'(T)$ (and equivalently $\chi''(T)$) curves are shifted towards higher temperatures as the frequency increases reflecting the fact that the current density is proportional to ω ($J \sim \omega^{\frac{1}{n-1}}$ for a $E - J$ characteristic of the form: $E \sim J^n$).

Traditionally, creep phenomena in ac susceptibility are investigated by mapping out the shift of the temperature T_p corresponding to the maximum of dissipation (*i.e.* the maximum of χ'') with the frequency and/or amplitude of the driving field. The main drawback of this procedure is that it only makes use of one point of the $\chi''(T)$ curve (corresponding to $h_{ac}/J(T = T_p, \omega) \sim d$) and numerous temperature scans have thus to be performed for different h_{ac} values in order to reconstruct the $J(T)$ curve. On the other hand, this procedure is very general since it is independent of the nature of the ac response or sample geometry (*i.e.* the shape of the $F(x)$ function). However, the determination of the $F(x)$ function (see Sect. 3) makes possible to deduce directly $J(T)$ from one single $\chi'(T)$

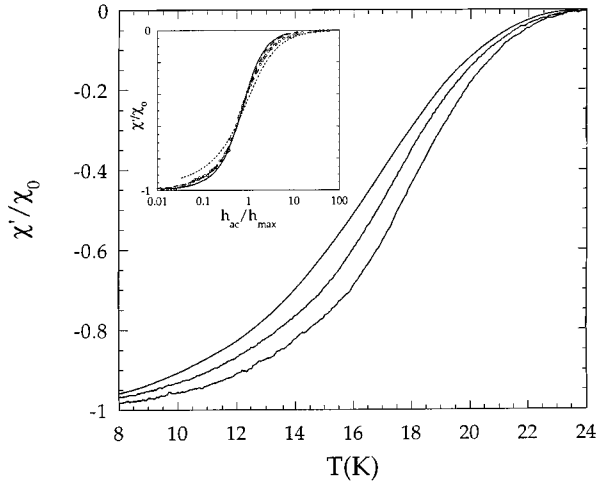


Fig. 3. Temperature dependence of the real part of the susceptibility of the (K, Ba)BiO₃ thick film at three different frequencies (from left to right $\omega = 0.02, 2$ and 2000 Hz). In the inset h_{ac} field dependence of χ' (same as Fig. 1). The solid, dashed and dotted lines are the theoretical calculations for creep exponents $n = 51, 11$ and 5 respectively.

scan by inverting equation (1):

$$J(T, \omega) = \frac{h_{ac}}{dF'^{-1}(\chi'(T, \omega))}. \quad (2)$$

Such a procedure has for instance been used recently by Jonsson *et al.* [22] in thin Hg – 1212 films in the large h_{ac}/J limit for which $F'(x) \sim x^{-3/2}$.

The temperature dependence of the current density deduced from $\chi'(T)$ following equation (2) is shown in the inset of Figure 4 (note that we obtained a very good agreement between the as-deduced $J(T)$ values and those obtained from the traditional “shift of the χ'' maximum” method (at $\omega = 12$ Hz)) and the corresponding frequency dependence of J (renormalized at 0.02 Hz) has been reported in Figure 4 at $T = 14, 18$ and 22 K. As shown, $J(\omega)$ can be well described by a power-law behaviour on the entire frequency range. This behaviour suggests that the activation energy U is of the form: $U_0 \ln(J/J_0)$ as first proposed by Zeldov *et al.* in BiSrCaCuO [17]. J is then expected to be proportional to $\omega^{\frac{kT}{U_0}}$ and the corresponding relaxation rate $S = d \ln(J) / d \ln(\omega)$ is hence equal to $kT/U_0 \sim 4\%$ at $H_{dc} = 0.3T$. Surprisingly this value is very similar to the one obtained in high T_c cuprates [1] and almost temperature independent. As pointed out by Malozemoff *et al.* [23], such a universality can be hardly understood in $U \sim \ln J$ model for which S is expected to be both temperature and sample (*i.e.* U_0) dependent but naturally comes out in the collective creep and/or vortex glass theory ($U \sim J^{-\mu}$) for which $S = 1/\mu \ln(1/\omega\tau)$ where τ is a macroscopic time scale. In this latter model S depends only on the creep exponent μ and is thus expected to be both sample and temperature independent for a given μ value (the frequency dependence can be neglected for $\omega \ll 1/\tau$ and $\ln(1/\omega\tau) \sim 20$ for $\tau \sim 10^{-9}$ s).

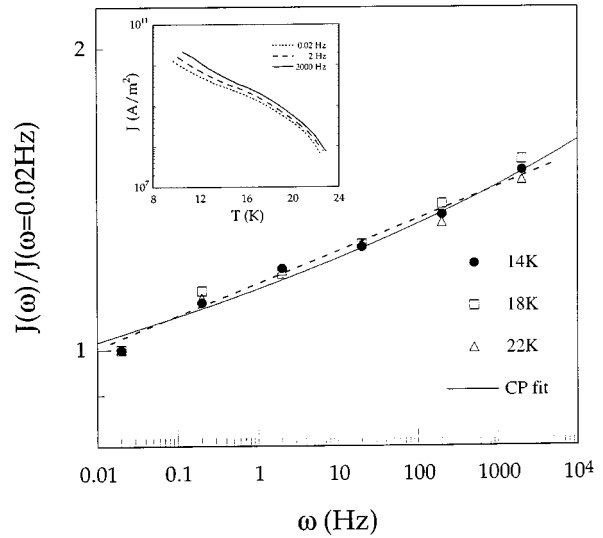


Fig. 4. Frequency dependence of the current density of the (K, Ba)BiO₃ thick film (renormalized at 0.02 Hz) at different temperatures. The solid line is a collective creep fit to the data in the small bundle regime. The dotted straight line is expected for an activation energy of the form $U \sim \ln(J)$. In the inset: temperature dependence of the current density at various frequencies deduced from $\chi'(T)$ using equation (2).

In this model J is expected to scale as $\frac{1}{\ln(1/\omega\tau)^{1/\mu}}$ and reasonable good fits to the data can actually be obtained assuming that $\mu = 3/2$ *i.e.* in the so-called small-bundle regime (see solid line in Fig. 4). It is thus very difficult to draw any definitive conclusion on the creep model from the frequency dependence of the current density. Note that, at higher fields (see [15] at $H_{dc} = 2T$) the relaxation rate becomes strongly temperature dependent and rises up very rapidly as the vortex-glass transition line is approached. We have even shown that $J(T)$ is completely dominated by the temperature dependence of S in the vicinity of the transition [15] (μ decreases towards ~ 0.2 as the transition line is approached). The major difference between those previous measurements and the present data is the amplitude of the external dc field. Indeed, we have shown by Small Angle Neutron Scattering that the vortex lattice is well ordered at low field [24] and it is thus very reasonable to assume that the creep effects are dominated by collective elastic deformations in this field limit. At higher fields the structure becomes disordered and plastic deformation may play a crucial role leading to a temperature and field dependent μ value (the “collective” nature of the creep in this regime is still an open question [25]). A more detailed study of the temperature and magnetic field dependence of the relaxation is under investigation and will be published in a forthcoming paper.

5 Conclusion

We have performed a detailed characterization of the ac susceptibility on (K, Ba)BiO₃ samples with different

geometrical shapes. The response of vortices to ac excitations is in good agreement with recent numerical calculations in the *bulk* pinning regime. The T and ω dependences of the current density have been directly deduced from the temperature scans of the susceptibility at various frequencies. The relaxation rate S is almost temperature and frequency independent $\sim 4\%$ at $H_{dc} = 0.3T$. A frequency independent S value is suggesting that the activation energy is of the form $U \sim \ln(J)$ eventhough collective creep effects cannot be excluded.

A. Conde-Gallardo thanks the CONACYT-Mexico for financial fellowship.

References

1. Y. Yeshurun, A.P. Malozemoff, A. Shaulov, *Rev. Mod. Phys.* **68**, 911 (1996).
2. J.R. Clem, A. Sanchez, *Phys. Rev. B* **50**, 9355 (1994).
3. E.H. Brandt, M.V. Indenbom, A. Forkl, *Europhys. Lett.* **22**, 735 (1993).
4. L. Ji, H. Sohn, G.C. Spalding, C.J. Lobb, M. Tinkham, *Phys. Rev. B* **40**, 10936 (1989).
5. E. Zeldov, A.I. Larkin, V.B. Geshkenbein, M. Konczykowski, D. Majer, B. Khaykovich, V.M. Vinokur, H. Shtrikman, *Phys. Rev. Lett.* **73**, 1428 (1994).
6. J. Gilchrist, M. Konczykowski, *Physica C* **212**, 43 (1993).
7. M. Wurlitzer, F. Mrowka, P. Esquinazi, K. Rogacki, B. Dabrowski, E. Zeldov, T. Tanegai, S. Ooi, *Z. Phys. B* **101**, 561 (1996).
8. C.J. van der Beck, M.V. Indenbom, G. D'Anna, W. Benoit, *Physica C* **258**, 105 (1996).
9. M. Wurlitzer, M. Lorenz, K. Zimmer, P. Esquinazi, *Phys. Rev. B* **55**, 11816 (1997).
10. E.H. Brandt, *Phys. Rev. B* **55**, 14513 (1997).
11. E.H. Brandt, *Phys. Rev. B* **58**, 6523 (1998).
12. M.J. Qin, X.X. Yao, *Phys. Rev. B* **54**, 7536 (1996).
13. T. Klein, A. Conde-Gallardo, J. Marcus, C. Escribe-Filippini, P. Samuely, P. Szabo, A.G.M. Jansen, *Phys. Rev. B* **58**, 12411 (1998).
14. W. Harneit *et al.*, *Physica C* **267**, 270 (1996); W. Harneit *et al.*, *Europhys. Lett.* **36**, 141 (1996).
15. T. Klein, W. Harneit, I. Joumard, J. Marcus, C. Escribe-Filippini, D. Feinberg, *Europhys. Lett.* **42**, 79 (1998).
16. P. Samuely, P. Szabo, T. Klein, A.G.M. Jansen, J. Marcus, C. Escribe-Filippini, P. Wyder, *Europhys. Lett.* **41**, 207 (1998).
17. E. Zeldov, N.M. Amer, G. Koren, A. Gupta, M.W. McElfresh, R.J. Gambino, *Appl. Phys. Lett.* **56**, 680 (1990).
18. M.V. Feigel'man, V.B. Geshkenbein, A.I. Larkin, V.M. Vinokur, *Phys. Rev. Lett.* **63**, 2303 (1989).
19. R. Prozorov, A. Shaulov, Y. Wolfus, Y. Yeshurun, *J. Appl. Phys.* **76**, 11 (1994).
20. Very similar $F(x)$ functions are obtained in the $h_{ac} \gg Jd$ limit reflecting the fact that the minor hysteretic loop becomes almost parallelogrammic for large h_{ac} values whatever the geometry or the pinning model.
21. taking the lowest thickness over width ratio which has been reported in [11]: $a/d = 0.03$
22. B.J. Jonsson, K.V. Rao, S.H. Yun, U.O. Karlsson, *Phys. Rev. B* **58**, 5862 (1998).
23. A.P. Malozemoff, M.P.A. Fisher, *Phys. Rev. B* **42**, 6784 (1990).
24. I. Joumard, J. Marcus, T. Klein, R. Cubitt, *Phys. Rev. Lett.* **82**, 4930 (1999).
25. T. Klein, W. Harneit, L. Baril, C. Escribe-Filippini, D. Feinberg, *Phys. Rev. Lett.* **79**, 3795 (1997).